

# Effects of saline water irrigation on soil properties in northwest China

Cui Hua Huang · Xian Xue · Tao Wang ·  
Roberto De Mascellis · Giacomo Mele ·  
Quan Gang You · Fei Peng · Anna Tedeschi

Received: 23 December 2009 / Accepted: 30 August 2010 / Published online: 22 September 2010  
© Springer-Verlag 2010

**Abstract** Due to the lack of freshwater, highly saline groundwater was the main irrigation source in the last few decades in the Minqin Basin, which is in northwest China. The study evaluates the effects of salt accumulation on the soil physical–chemicals properties. Undisturbed and disturbed soil samples were taken from the experiment site, which was irrigated with saline water at a concentration of 0.8, 2 and 5 g L<sup>-1</sup> (coded later as C<sub>08</sub>, C<sub>2</sub> and C<sub>5</sub>). Undisturbed soil samples, at depths of 0–45 and 45–60 cm were taken to determine the water retention curve (WRC). Moreover, in the same place, another set of undisturbed soil samples were taken to determine the porosity and pore-size distribution (PoSD). From the WRC, the water-holding capacity of the soil was estimated. Disturbed soil samples at depths of 0–20, 0–45, 45–60 and 80–100 cm were taken to determine the index of aggregates stability in water (IC). The electrical conductivity of the saturated paste (EC<sub>e</sub>) was determined at depths of 0–30, 30–60 and 60–90 cm, during the irrigation season on C<sub>08</sub>, C<sub>2</sub> and C<sub>5</sub> treatments. The results show that the total porosity and the index of aggregates stability in water decrease with the increasing salinity of irrigation water, and the EC<sub>e</sub> increases with the

increasing salinity of irrigation water especially in the surface soil. The water-holding capacity (WHC) of soil also increases with the increasing salinity of irrigation water.

**Keywords** Saline water irrigation · Soil porosity · Index of aggregates stability in water · Water-holding capacity

## Introduction

Saline water is used to irrigate croplands in different parts of the world, especially in arid and semi-arid regions, which occupy 41% of the global land surface (UNDP 1997), with poor water quantity and quality. In these regions, the limited rainfall (<400 mm/year) is not sufficient to leach out salts from the root zone, which leads salt from the irrigation water to accumulate in the soil and affect the soil properties. Literature shows that the concentration of sodium, calcium and magnesium ions in soil layers can affect the dispersion of clay particles, the soil hydraulic conductivity (Shainberg and Letey 1983), soil aggregate stability and the formation of soil crusts (Varallyay 1977a, b; Tedeschi and Dell' Aquila 2005). Dispersion of soil particles may cause clogging of soil pores, which reduces the soil permeability, soil porosity and soil hydraulic conductivity (Felhendler et al. 1974; Frenkel et al. 1978; Pupisky and Shainberg 1979; Shainberg et al. 1981a, b; Shainberg and Levy 1992; Amézketa 1999). Therefore, drought and salinization are two main factors affecting the arid irrigated agriculture (Tedeschi et al. 2007). In addition, irrational human activities, such as poor agricultural management, flood irrigation and so on, also aggravate salinization, due to ineffective control of the accumulation of salts in soil. Therefore, salinity increases

C. H. Huang · X. Xue · T. Wang (✉) · Q. G. You · F. Peng  
Key Laboratory of Desert and Desertification,  
Cold and Arid Regions Environmental and Engineering  
Research Institute, Chinese Academy of Sciences,  
320 West Donggang Road, Lanzhou 730000, China  
e-mail: wt@lzb.ac.cn

C. H. Huang · F. Peng  
Graduate School of Chinese Academy of Sciences,  
Beijing 100039, China

R. De Mascellis · G. Mele · A. Tedeschi  
Institute for Agricultural and Forest Mediterranean Systems,  
CNR, Via Patacca 85, Ercolano, 80056 Naples, Italy

in extensive portions of irrigated lands, which become degraded by salinization (Ghassemi et al. 1995).

Saline water is not beneficial to irrigated agriculture, but it may still be the major irrigation water source in extensive arid regions, especially in developing countries where extreme shortage of freshwater and the rapidly increasing population require more water. For example, in Minqin Basin of northwest China, the local population increased from  $20.8 \times 10^4$  in 1950 to  $30.2 \times 10^4$  in 2004, the area of croplands increased from  $3.0 \times 10^4$  ha in the 1950s to  $5.3 \times 10^4$  ha in 2001, and yearly freshwater supply decreased from  $5.14 \times 10^8$  m<sup>3</sup> in 1956 to  $0.65 \times 10^8$  m<sup>3</sup> in 2004. For sustaining the existing croplands and guaranteeing subsistence, local farmers have to exploit the groundwater with high salinity to irrigate croplands, which leads to salt accumulation in the soil under strong evaporation. Soil salinization results in the dry out of vegetation, desertification, land encroachment and environmental degradation (Wang and Cui 2004).

The negative impact of saline irrigation water can be mitigated by implementing appropriate management of saline water and soil, which requires a better understanding of how soil properties are affected by the irrigation system, water management strategies, irrigation frequency, etc., and when to use saline water to irrigate arid croplands. The aim of this work was to study the effects of saline water irrigation on soil properties.

## Materials and methods

### Study area

The study area, Minqin Basin, which spreads in the lower reach of Shiyang River in northwest China, is an alluvial plain affected by soil and groundwater salinity throughout the basin, with the geographical position of 103°02'E–104°02'E and 38°05'N–39°06'N (Fig. 1). The Shiyang River originates from Qilian Mountain with an altitude of 2,000–5,000 m above sea level and an alpine climate. The middle reach of Shiyang River flows through the Liangzhou Oasis and Jinchang Oasis with an altitude of 1,400–2,000 m and a semi-arid temperate climate. The downstream reach of the Shiyang River flows into the Minqin Oasis at an altitude of 1,000–1,400 m and with an arid temperate climate (Ma et al. 2005), and then disappears into the desert.

Climate change and overuse of water sources in the upper and middle reaches of Shiyang River result in the rapid reduction of water flowing into the lower reach, which forces the local farmers to overexploit the groundwater in the Minqin Basin. The annual runoff flowing into the Minqin Basin was  $5.73 \times 10^8$  m<sup>3</sup> during the 1950s (Zhu et al. 2007) and  $<1 \times 10^8$  m<sup>3</sup> at present. The annual

average exploitation amount of groundwater in the Minqin Basin was  $<1.0 \times 10^8$  m<sup>3</sup> before 1970s and reached  $6.65 \times 10^8$  m<sup>3</sup> in 2003; the mean increasing rate was  $0.2 \times 10^8$  m<sup>3</sup>/year (GSWRB 2007). Based on the research of Chang and Zhao (2006), the groundwater table of the experiment site and the surrounding area was 1–3 m in the 1950s and reached 16.4–22.2 m by the end of 2004. In the north of Minqin Basin, adjacent to the Tenger desert (Fig. 1), the groundwater quality is poor because of the overuse of groundwater, strong evaporation and lack of surface freshwater recharge; the total dissolved solids (TDS) of groundwater can reach 10 g L<sup>-1</sup> (GSWRB 2007).

Flood and/or furrow irrigation are dominant irrigation methods in study area; both of them are widely used water irrigation methods and can accelerate soil salinization and degradation. As a result of irrigation with alkali-saline groundwater and poor agricultural management, the phenomena of soil salinization have increased significantly in recent decades (Ma and Wei 2003). In Minqin Basin, the average salt content of the soil is up to 16.7 g kg<sup>-1</sup> and most farmlands can no longer be used for cultivation due to salinization.

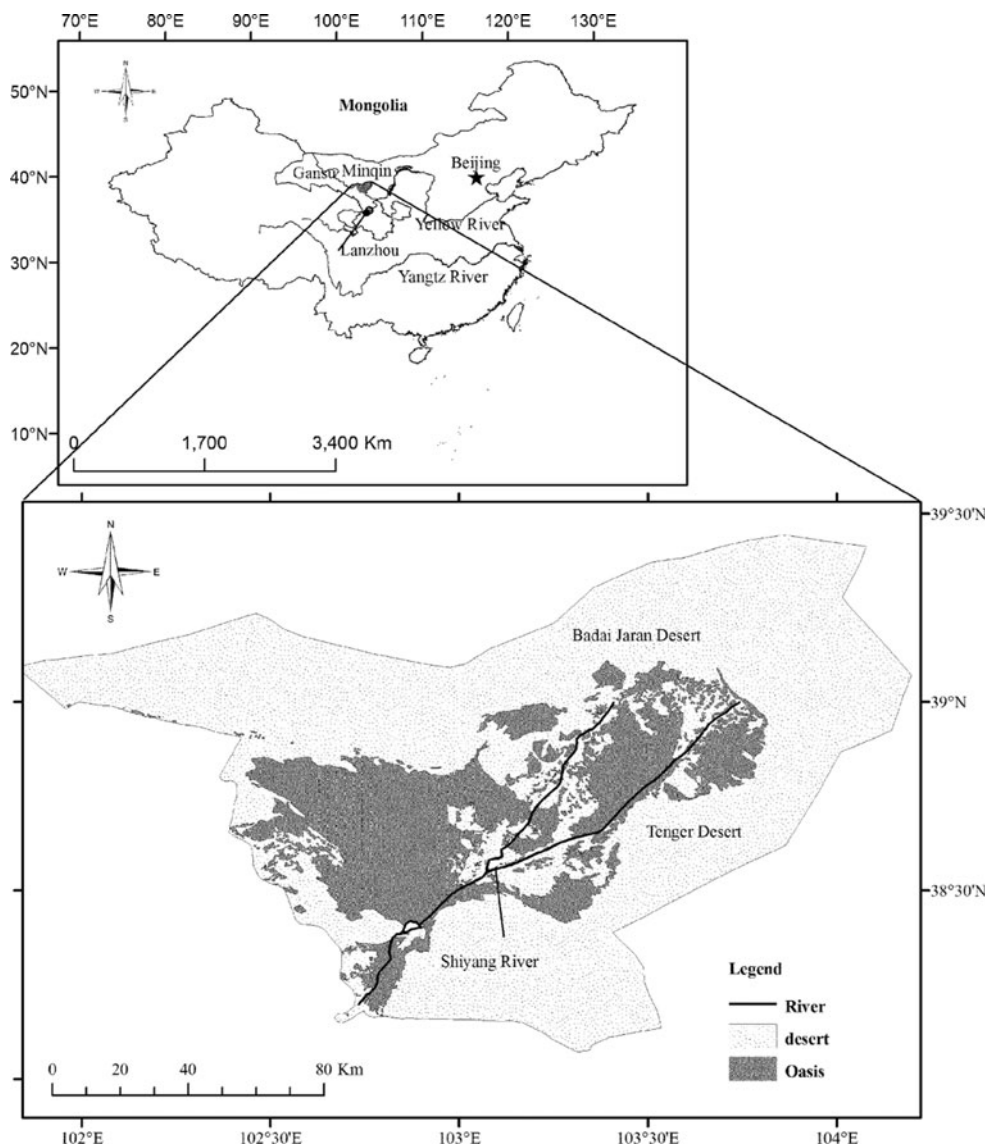
### Experiment site

The study was conducted in Minqin Desert Control Station, which is in the Minqin Basin of northwest China, with a geographical position of 103°59'E and 38°34'N. In the study area, solar resources are abundant and average sunshine hours is 3,021. Mean annual precipitation is 115 mm and almost 74% of that is recorded from June to September. Mean annual evaporation reaches 2,593 mm. Mean daily temperature is 7.7°C. Mean wind speed is 2.4 m s<sup>-1</sup> and the maximum wind speed reaches 23.0 m s<sup>-1</sup>. Average air humidity is 49% and aridity is 5.3 (Zhao et al. 2003). The average frost-free period is 173 days and the longest one is 202 days. The soil is silty loam, as reported in Table 1. The complete composition of the ion exchange complex in different layers of the experimental field is given in Table 2.

In the experiment site, there was a control treatment (C<sub>08</sub>, 0.8 g L<sup>-1</sup>) and two salinity treatments, C<sub>2</sub> and C<sub>5</sub>, respectively, with water concentrations of 2 and 5 g L<sup>-1</sup>. Table 3 shows the ionic compositions of the irrigation water for which all the treatments were replicated four times.

### Soil sampling

To evaluate the effects that salt accumulation has on the change of the soil physical and chemical properties, disturbed and undisturbed soil samples were taken in 2007 to determine the following: porosity and pore-size-distribution

**Fig. 1** Location of the study area**Table 1** Soil texture of C<sub>08</sub>, C<sub>2</sub> and C<sub>5</sub>

Treatments	Clay (%)	Silt (%)	Sand (%)
C <sub>08</sub>	13.07	41.14	45.80
C <sub>2</sub>	21.16	59.11	19.75
C <sub>5</sub>	15.25	50.43	34.33

**Table 2** Exchangeable cations of experimental farm

Soil layer depth (cm)	Exchangeable cations ( $\text{g kg}^{-1}$ )				
	Total	$\text{Ca}^{2+}$	$\text{Mg}^{2+}$	$\text{K}^+$	$\text{Na}^+$
0–20	0.39	0.06	0.07	0.08	0.06
20–40	0.41	0.07	0.08	0.09	0.04
40–60	0.41	0.07	0.08	0.10	0.02
60–80	0.39	0.06	0.07	0.12	0.02
80–100	0.36	0.06	0.06	0.11	0.02

(PoSD); water retention curve (WRC); the aggregate stability in water (IC) and the electrical conductivity of the saturated paste (EC<sub>e</sub>).

#### Undisturbed samples

**Porosity and pore-size-distribution (PoSD)** Undisturbed soil samples from the top layer were taken to determine the total porosity and the PoSD. Two samples for each area were collected using aluminium cylinders, 12 cm in height and with a diameter of 10 cm. The undisturbed samples were then impregnated with a polyester resin in which a fluorescent dye was added and the samples were treated afterwards as reported in Mele (2001) to obtain the sections for image acquisition. The digital images of the four faces of each sample were acquired at a resolution of 30  $\mu\text{m}/\text{pixel}$ . Each dimension of the four faces of the samples, on

**Table 3** Chemical composition and sodium absorption rate (SAR) of irrigation water for C<sub>0.8</sub>, C<sub>2</sub> and C<sub>5</sub>

Ions (mg L <sup>-1</sup> )	C <sub>0.8</sub>	C <sub>2</sub>	C <sub>5</sub>
Cl <sup>-</sup>	120	323	890
SO <sub>4</sub> <sup>2-</sup>	225	739	1,640
HCO <sub>3</sub> <sup>-</sup>	296	307	360
CO <sub>3</sub> <sup>2-</sup>	0	14	0
Ca <sup>2+</sup>	87	126	280
Mg <sup>2+</sup>	44	192	190
K <sup>+</sup>	5	229 <sup>a</sup>	1,000 <sup>a</sup>
Na <sup>+</sup>	52		
TDS	0.8	2.0	5.0
SAR (mmol <sup>1/2</sup> L <sup>-1/2</sup> )	1.6	4.2	15.9
pH	8.0	8.0	7.5
Ec (dS m <sup>-1</sup> )	1.16	2.64	7.03

<sup>a</sup> The value reported in the table for Na and K for the treatment C<sub>2</sub> and C<sub>5</sub> is the sum of the two cations

which 2D image analysis was carried out, was 11 cm × 5.5 cm. The image analysis was performed according to the procedure described by Moreau (1997) and Mele et al. (1999). The image analysis was used to determine the following measurements:

- (1) Vertical profiles of porosity, i.e. porosity plotted against the soil depth up to 12 cm. This measure enabled the evaluation of the possible presence and degree of soil compaction;
- (2) PoSD evaluated by mathematical morphology algorithms (Serra 1982; Horgan 1998) with the aim to obtain more detailed quantitative information on the soil structure changes due to the specific treatments considered.

**Water retention curve (WRC)** Undisturbed soil samples were taken at 0–45 and 45–60 cm with aluminium cylinders ( $\phi = 8.6$  cm,  $h = 13.0$  cm), to determine the (WRC)  $h(\theta)$  in the laboratory according to the procedure suggested by Tamari et al. (1993). The soil water retention characteristics have been parameterized using the relationship proposed by Van Genuchten (1980) and by Ross and Smettem (1993). The parameters of the retention functions were obtained by a least squares optimisation technique and were used to calculate available water retention capacity at prescribed pressure head values.

From (WRC)  $h(\theta)$ , the wilting point and the field capacity were estimated to evaluate the soil water-holding capacity (WHC). The WHC can be a support to describe

and assess the soil water balance such as partition between infiltration, runoff and evaporation, and therefore to improve irrigation management especially under drought and salinity conditions.

#### Disturbed samples

**Aggregate stability in water** Disturbed soil samples at a depth of 0–20 cm and another set with intervals of 0–45, 45–60 and 80–100 cm for each treatment were taken and the aggregate stability in water was measured, replicated twice and the average value was considered.

The soil samples were air dried and mashed at two diameters range. One part of soil samples was mashed and sieved in aggregates with diameters in the 4.75–2 mm range, and the other in aggregates with diameters in the 2–1 mm range. The aggregate stability in water was measured by an apparatus developed at the Institute for Agricultural and Forest Systems in the Mediterranean (Ercolano, Naples) (Tedeschi and Dell'Aquila 2005; Dell'Aquila 2007), which works by vertical oscillation. The measurements were performed on 10 g of soil aggregates with a diameter in the range of 2–1 and 4.75–2 mm. According to Tedeschi (1999) aggregates were non-wetted and shaken at a speed of 30 cycles/min with a sieve stroke length of 3 cm. The index of aggregate stability was expressed by the following IC equation (Pagliai 1997), which is more suitable to soil in which a high sand fraction is present.

$$IC = 100 \times \left( \frac{C - CS}{D - CS} \right)$$

$C$  means aggregates not dispersed after 30 min and  $CS$  means coarse sand;  $D$  means quantity of soil sample used for the determination.

**Electrical conductivity of the saturated paste (EC<sub>e</sub>)** During the irrigation season, soil samples at a depth of 0–30, 30–60 and 60–90 cm on each of the four repetitions were taken to determine the electrical conductivity of the saturated paste (EC<sub>e</sub>) according to Rhoades (1996). Due to the large amount of soil to be analysed, the determination of EC<sub>1:2.5</sub> was carried out because the preparation of a solution in which 10 g of soil is mixed with 250 ml of water is less time consuming than for water-saturated samples. For a limited number of samples, the EC<sub>e</sub> was also determined. Then, a linear regression  $EC_e = a + b (EC_{1:2.5})$  for each layer was established, significant at  $p < 0.01$ . The EC<sub>e</sub> was finally estimated for all layers using this regression equation.

**Fig. 2** Image of vertical sections of soil pores, 0–11 cm deep

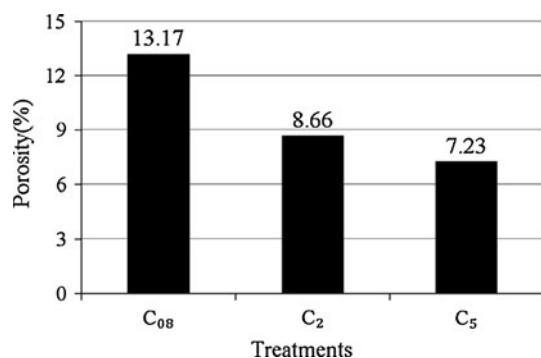
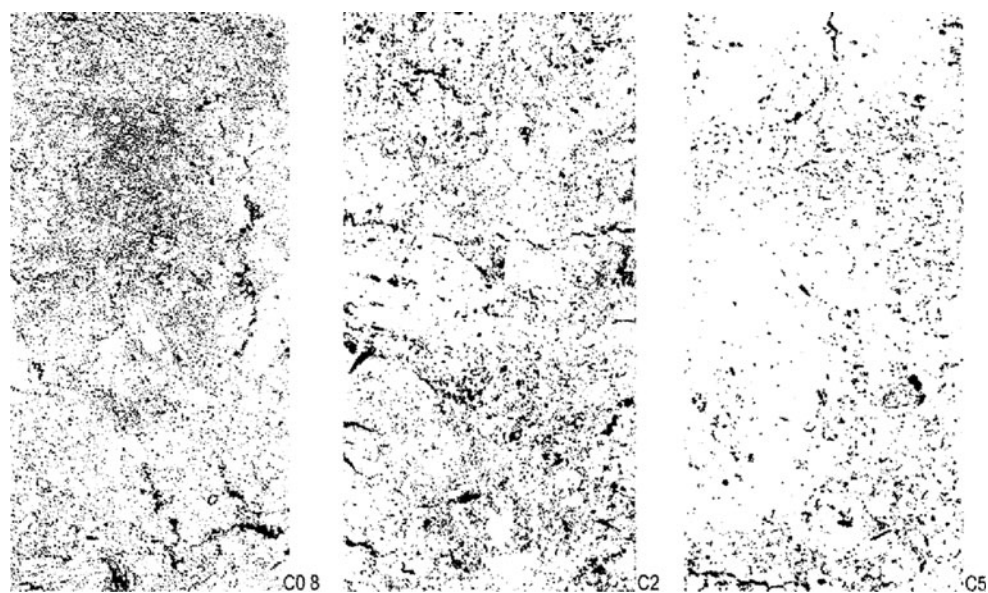


**Fig. 3** Porosity calculated from image analysis for C<sub>08</sub>, C<sub>2</sub> and C<sub>5</sub>

## Results and discussion

### Porosity and pore-size distribution (PoSD)

Figure 2 shows the images of vertical sections of undisturbed samples from the upper 11 cm of soils in the three treatments of C<sub>08</sub>, C<sub>2</sub> and C<sub>5</sub> separately. The black part is soil pore; the white part is the solid phase. Averaged values of eight images (two samples) for each soil are reported in Figs. 3, 4 and 5. These results refer only to the pores larger than 30 µm due to the limited image resolution. Figure 3 shows that porosity is closely related to water salinity, and decreases from 13.17% for C<sub>08</sub> to 7.23% for C<sub>5</sub>. The vertical porosity profile of the upper 11 cm in Fig. 4 shows that the porosity reduction has occurred mainly in the upper 5 cm on the treatments C<sub>2</sub> and C<sub>5</sub>. Comparison of PoSD demonstrates that except for C<sub>08</sub>, a reduction of pores larger than 240 µm (Fig. 5) occurred at increasing soil salinity level. The different behaviour of PoSD for C<sub>08</sub> is strictly related to the completely different pore architecture

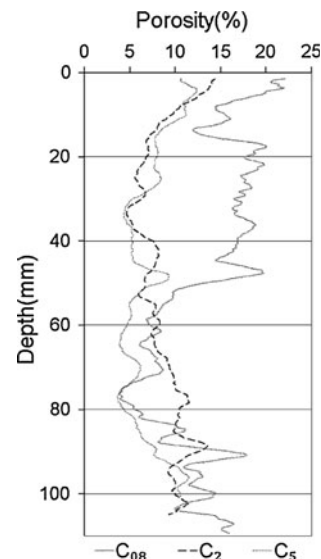


**Fig. 4** Porosity comparison of C<sub>08</sub>, C<sub>2</sub> and C<sub>5</sub> for the upper 11 cm

found in the analysed sample, which shows an abundance of small homogeneous pores in the upper 5 cm and a compact layer under that depth (Figs. 2, 4).

The observed difference in porosity and PoSD confirms that, at least in the upper 11 cm and in the largest pore-size spectrum, the soil structure was affected by the saline water.

### Soil aggregation stability in water

Table 4 reports the aggregate stability in water, for both the aggregates classes, i.e. in the range 4.75–2 and 2–1 mm, expressed by the IC (%) index for the top soil layer (0–20 cm). The IC for both aggregate sizes decreases as

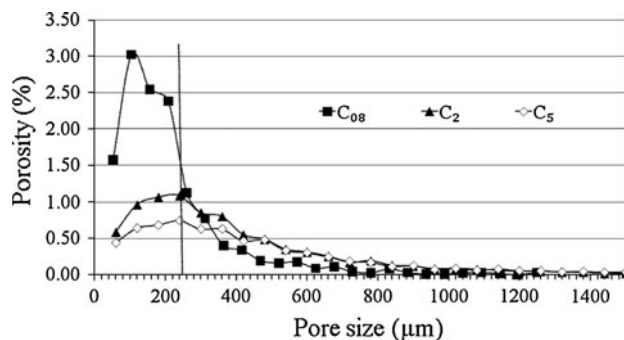


**Fig. 5** Pore size distribution for  $C_{08}$ ,  $C_2$  and  $C_5$

**Table 4** Aggregate stability index (IC) for the soil treatments of  $C_{08}$ ,  $C_2$  and  $C_5$  at surface soil

Treatment	Depth (cm)	Aggregate 4.75–2 mm IC (%)	Aggregate 2–1 mm IC (%)
$C_{0.8}$	0–20	16.6	6.75
$C_2$	0–20	12.6	6.4
$C_5$	0–20	7.5	2.3

salinity increases. The trend is the same for the different classes of aggregates considered. In Fig. 6, the index of aggregate stability in water (IC) is reported for aggregates of 4.75–2 mm and is significantly lower for  $C_5$  at all depths and higher for  $C_{08}$ . IC of  $C_2$  is between those of  $C_{08}$  and  $C_5$  at all layers. It is interesting to note that the IC of  $C_{08}$  for all layers has the highest aggregate stability even if it decreases at a depth of 55 cm. This trend is observed also in the other treatments even if they are small. The 55 cm is the tillage layer, and soil compaction occurred in all soils considered, but it is important to maintain the trend.

The results are in agreement with that of Tedeschi and Dell' Aquila 2005, who found a decrease in the index of aggregate soil stability in water at increasing soil salinity.

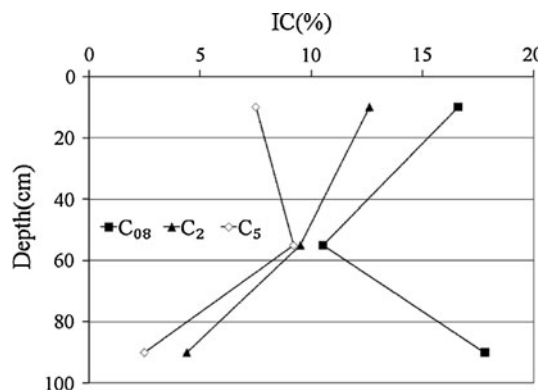


**Fig. 6** Aggregates stability indexes of  $C_{08}$ ,  $C_2$  and  $C_5$

**Table 5** Water-holding capacity (WHC) in the root zone (0–60 cm)

Treatments	WHD (mm)
$C_{08}$	87.82
$C_2$	143.13
$C_5$	116.01

#### Water-holding capacity (WHD)

The observed increase (Table 5) of WHD (range between field capacity and wilting point) is apparently in agreement with the trend observed in the soil structure (PoSD and IC). The fraction of pore space at smaller pore diameters decreases, whilst the contribution of larger pores increases. This change in WHD is most relevant to irrigation management under saline condition, as better knowledge of the water-holding capacity (WHD) helps to decide when and how much irrigation water should be applied. Such results can have an important impact on the quantity of water distributed by irrigation, because due to the higher storage capacity it would be possible to apply water at longer irrigation intervals, e.g. to deal with long and regular rotational intervals.

#### Electrical conductivity ( $EC_e$ )

The leaching irrigation applied before sowing determined an  $EC_e$  around  $4.0 \text{ dS m}^{-1}$  (Fig. 7) for all the treatments and for the first 60 cm (0–30 and 30–60 cm), whilst for the deepest layer and for all the treatments the  $EC_e$  was  $<3.5 \text{ dS m}^{-1}$ .

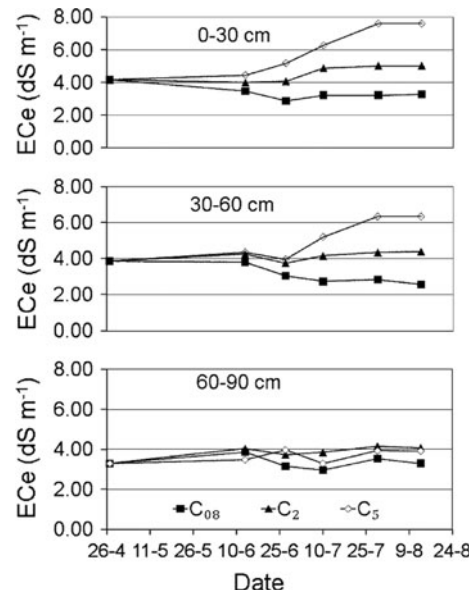


**Fig. 7**  $EC_e$  of  $C_{08}$ ,  $C_2$  and  $C_5$  in the whole growing season

The EC<sub>e</sub> values measured after each irrigation show how salt accumulation occurred especially in the layers 0–30 and 30–60 cm. The EC<sub>e</sub> values increase with increasing concentration of the applied saline irrigation water. At the end of the irrigation season, a progressive increase of EC<sub>e</sub> occurred especially for the C<sub>2</sub> (EC<sub>e</sub> = 5 dS m<sup>-1</sup>) and C<sub>5</sub> (EC<sub>e</sub> = 7.6 dS m<sup>-1</sup>) treatments for the layers 0–30 and 30–60 cm (respectively, EC<sub>e</sub> = 4.3 and 6.34 dS m<sup>-1</sup> for C<sub>2</sub> and C<sub>5</sub>). The EC<sub>e</sub> for the treatment C<sub>08</sub> was almost around the same value throughout the season in the layer 0–30 cm (EC<sub>e</sub> = 3.2 dS m<sup>-1</sup>). In the layer 30–60 cm and for the C<sub>08</sub>, a slight decrease of EC<sub>e</sub> values occurred (EC<sub>e</sub> = 3.0 dS m<sup>-1</sup>). In the deepest layer, 60–90 cm, a slight increase of EC<sub>e</sub> for the C<sub>2</sub> and C<sub>5</sub> treatments was observed compared with the EC<sub>e</sub> observed in the C<sub>08</sub> treatment. Nevertheless, the salt accumulation in this layer was lower than that observed in the layers above. This confirms that irrigation management did not determine a large salt leaching to the deepest layer, thus reducing the risk of leaching a significant salt amount into the groundwater. However, the risk that the winter rainfall and the irrigation applied before the next sowing can leach the salt at later stage remains.

The soil layer most affected by salinity is the 60 cm deep layer, where most roots are located, i.e. with a significant risk of lower crop production.

## Conclusions

It can be concluded that the results of the present study of the soil physical changes due to the effects of saline irrigation have determined a salt accumulation (EC<sub>e</sub>) in the soil profile, with higher EC<sub>e</sub> in the first 60 cm soil depth for the C<sub>2</sub> and C<sub>5</sub> treatments. The accumulation increases with time during the application of saline water.

Several studies (Shainberg and Levy 2004; Rengasamy et al. 1996; Shainberg and Letey 1983; Minhas and Sharma 1986) have reported how salt accumulation causes the deterioration and deflocculation of the clay colloids with destruction in aggregates and soil structure and clogging of macro pores, accompanied by unfavourable consequences on the soil hydrological properties. In this study, the soil structure expressed by IC, which decreases with increasing salinity, showed deterioration along the whole soil profile, clearly as a result of the deflocculation of clay colloids induced by the salt.

According to Quirk (1986) and Quirk and Schofield (1955), the clay flocculation due to the salt concentration can cause a reduction in porosity. High levels of salinity, therefore, induce a replacement of pores of larger diameters with pores of smaller diameters that explain the increase of total porosity captured in this study.

In the context of irrigation water management, observed changes in WHC are particularly relevant, as a better knowledge of WHC leads to more accurate irrigation schedules optimised on the basis of WHC and the water retention characteristics. The latter helps to reduce water and salinity stress by keeping soil water content closer to field capacity for longer periods of time.

**Acknowledgments** The authors would like to thank Dr. A. Basile for the careful comments, Miss N. Orefice for performing the hydrological measurements on the undisturbed soil samples, Mr. B. Di Matteo for performing the porosity and image analysis measurements, and Dr. M. Riccardi for performing the chemical analysis. The author also expresses particular thanks to Gansu Minqin National Studies Station for Desert Steppe Ecosystem for providing meteorological data and caring during the field experiment. This study was supported by funds from the National Natural Science Foundation of China (30870412), West Light Foundation of the Chinese Academy of Sciences (O728551001) and Ministry of Science and Technology of China (2009CB421308). Moreover, it was supported also by scientific bilateral cooperation 2004–2007/2008–2010 between CNR/Chinese Academy of Science and by the Short Term Mobility program funded by CNR 2007–2008.

## References

- Amézketa E (1999) “Soil aggregate stability: a review”. *J Sust Agric* 14:83–151
- Chang ZF, Zhao M (2006) Study on desert ecology in Minqin. Gansu Science and Technology Pub House, Gansu, pp 7
- Dell'Aquila R (2007) Automatic Sieve-Shaker for determining soil aggregate stability and dimensional distribution using vertical oscillation system. *Ital J Agron* 4(2):401–406
- Felhendler R, Shainberg I, Frenkel H (1974) “Dispersion and hydraulic conductivity of soils in mixed solution”. In: Transactions of the 10th international congress of soil science (Moscow). Nauka Pub. House, Moscow, pp 103–112
- Frenkel H, Goertzen JO, Rhoades JD (1978) Effects of clay type and content exchangeable sodium percentage, and electrolyte concentration on clay dispersion and soil hydraulic conductivity. *Soil Sci Soc Am* 42:32–39
- Ghassemi F, Jakeman AJ, Nix HA (1995) “Salinization of land and water resources: human causes, extent, management and case studies,” Cab International, 526
- GSWRB (2007) Shiyang River Basin major operation strategy. Gansu Province Water Resources Bureau, Gansu Lanzhou Government, pp 11–14
- Horgan GW (1998) Mathematical morphology for analysing soil structure from images. *Eur J Soil Sci* 49:161–173
- Ma JZ, Wei H (2003) The ecological and environmental problems caused by the excessive exploitation and utilization of ground-water resources in the Minqin Basin, Gansu Province. *Area Zone Res* 20(4):261–265
- Ma JZ, Wang XS, Edmunds WM (2005) The characteristics of ground-water resources and their changes under the impacts of human activity in the arid Northwest China—a case study of the Shiyang River Basin. *J Arid Environ* 61:277–295
- Mele G (2001) Proposta di una tecnica tomografica per l’analisi della struttura del suolo. *Riv Ing Agric* 2:93–100
- Mele G, Basile A, Leone AP, Moreau E, Terribile F, Velde B (1999) “The study of soil structure by coupling serial sections and 3D image analysis, modelling of transport processes in soils.” In:

- Feyen J, Wiyo K (eds) International workshop of EurAgEng's field of interest on soil and water, Leuven, pp 103–117
- Minhas PS, Sharma DR (1986) Hydraulic conductivity and clay dispersion as affected by application sequence of saline and simulated rain water. *Irrig Sci* 7(3):159–167
- Moreau E (1997) "Etude de la morphologie et de la topologie 2D et 3D d'un sol argileux par analyse d'images". PhD thesis. Université de Poitiers, France
- Pagliai M (1997) Metodi di analisi fisica del suolo. Ministero per le Politiche Agricole. Franco Angeli
- Pupisky H, Shainberg I (1979) Salt effects on the hydraulic conductivity of a sandy soil. *Soil Sci Soc Am J* 43:429–433
- Quirk PJ (1986) Soil permeability in relation to sodicity and salinity. *Phil Trans R Soc Lond A* 316:297–317
- Quirk PJ, Schofield RK (1955) The effects of electrolyte concentration on soil permeability. *Eur J Soil Sci* 6:163–178
- Rengasamy P, McLeod AJ, Ragusa SR (1996) Effects of dispersible soil clay and algae on seepage prevention from small dams. *Agric Water Manage* 29(2):117–127
- Rhoades JD (1996) Salinity: electrical conductivity and total dissolved solids. In: Spark DL (ed) Methods of Soil Analysis. Part 3. Chemical Methods, SSSA Book Series no. 5. ASA and SSSA, Madison
- Ross PJ, Smettem RJ (1993) Describing soil hydraulic properties with sums of simple functions. *Soil Sci Soc Am J* 57:26–29
- Serra J (1982) Image analysis and mathematical morphology. Academic Press, London
- Shainberg I, Letey J (1983) Response of soils to sodic and saline conditions. *Hilgardia* 52(2):1–57
- Shainberg I, Levy GJ (1992) "Physical-chemical effects of salts upon infiltration and water movement in soils" In: Wagenet RJ, Baveye P, Stewart BA (Eds) Interacting processes in soil science, pp 38–93
- Shainberg I, Levy GJ (2004) Flocculation and dispersion. Encyclopedia of Soils in the Environment, pp 27–34
- Shainberg I, Rhoades JD, Prather RJ (1981a) Effect of low electrolyte concentration on clay dispersion and hydraulic conductivity of a sodic soil. *Soil Soc Sci Am J* 45:273–277
- Shainberg I, Rhoades JD, Prather RJ (1981b) Effect of mineral weathering on clay dispersion and hydraulic conductivity of sodic soils. *Soil Soc Sci Am J* 45:287–291
- Tamari S, Bruckler L, Halbertsma J, Chadoeuf J (1993) A simple method for determining soil hydraulic properties in the laboratory. *Soil Sci Soc Am J* 57:642–651
- Tedeschi A (1999) Influence of soil sample conditioning in the evaluation of soil structure stability as affected by irrigation with saline water. *Ital J Agron* 3(2):117–122
- Tedeschi A, Dell' Aquila R (2005) Effects of irrigation with saline waters, at different concentrations on soil physical and chemical characteristics. *Agric Water Manage* 77:308–322
- Tedeschi A, Menenti M, Tedeschi P Wang T, Xue X, Basile A, Mele G, De Lorenzi F, De Mascellis R, Di Matteo B (2007) Design and evaluation of saline irrigation schedules to cope with droughts and scarce fresh water. In: Proceedings of ICID 22nd European regional conference: "water resources management and irrigation and drainage systems development in the European environment", Pavia, 2–6 September 2007
- UNDP (1997) Aridity zones and dryland populations. An assessment of population levels in the world's drylands. UNSO/UNDP, New York
- Van Genuchten MTh (1980) A closed form equation for predicting the hydraulic conductivity of unsaturated soils. *Soil Sci Soc Am J* 44:892–898
- Varallyay G (1977a) "Moisture states and flow phenomena in salt-affected soils." In: Proceedings of the Indo-Hung seminar on management of salt affected soils. Pergamon Press, Oxford, pp 85–102
- Varallyay G (1977b) Soil water problems related to salinity and alkalinity in irrigated lands. In: Arid land irrigation in developing countries. Pergamon Press, Oxford, pp 251–264
- Wang B, Cui XH (2004) Researches on laws of water balance at transitional zone between oasis and desert in Minqin. *Acta Acol Sin* 24(2):235–240
- Zhao M, Li AD, Wang YL (2003) A study on relations between transpiration of psammophyte and the meteorological components. *J Arid Land Resour Environ* 17(6):131–137
- Zhu GF, Li SS, Su HZ (2007) Hydrogeochemical and isotope evidence of groundwater evolution and recharge in Minqin Basin, Northwest China. *J Hydrol* 333:239–251